

FED-PV: A Large-Scale Synthetic Frame/Event Dataset for Particle-Based Velocimetry

Fan Wu, Xiang Feng, Aoyu Zhang, Yong Lee*

Hubei Provincial Engineering Research Center of Robotics & Intelligent Manufacturing, School of Mechanical and Electronic Engineering, Wuhan University of Technology, Wuhan 430070, China

* yonglee@whut.edu.cn

Abstract

Particle-based velocimetry (PV) is a widely used technique for non-invasive flow field measurements in fluid mechanics. Existing PV measurements typically rely on a single type of particle recording. With advancements in deep learning and information fusion, incorporating multiple different particle recordings presents a promising avenue for next-generation PV measurement techniques. However, we argue that the lack of cross-modal datasets—combining frame-based recordings and event-based recordings—represents a significant bottleneck in the development of fusion measurement algorithms. To address this critical gap, we developed a dual-modal data generator FED-PV to synthesize frame-based images and event-based recordings of moving particles, resulting in a 350GB dataset generated using our approach. This generator and dataset will facilitate advancements in novel PV algorithms.

1 Introduction

Particle-based velocimetry (PV) is a non-invasive flow field measurement technique widely used in experimental fluid dynamics, including particle image velocimetry (PIV) (Raffel et al., 2018; Lee et al., 2017b; Ai et al., 2025a), particle tracking velocimetry (PTV) (Ohmi and Li, 2000), event-based imaging velocimetry (EBIV) (Willert and Klinner, 2022), particle event velocimetry (PEV) (AlSattam et al., 2024). However, as the demands for higher performance, the limitations of single-modal PV methods have become apparent, making it challenging to improve the accuracy of measurements further (Kähler et al., 2012; Lee et al., 2024; Lee and Mei, 2021; Ai et al., 2025b). In particular, research on integrating multiple data sources, especially combining event-based data with particle image data, remains in its infancy and has yet to fully realize its potential (Wan et al., 2023). Thus, constructing a dual-modal particle velocity dataset not only fills the critical gap but also provides training/testing benchmarks for advancing PV technology in the coming measurement studies.

Constructing multimodal datasets (e.g., RGB and event data) is a common practice in the computer vision community. The datasets can be derived from real-world recordings (Zhu et al., 2018; Gehrig et al., 2021a) or generated using various simulation tools (Mueggler et al., 2017; Rebecq et al., 2018). However, these readily available datasets are rooted in real-world scenarios and cannot be directly applied to the PV area due to the domain gap. Due to the unknown latent flow fields, it is also challenging to obtain a large amount of dual-modal data with ground truth using real-world setups.

To overcome these limitations, we developed a particle frame/event generator and constructed a dual-modal particle flow dataset with ground truth. Specifically, the flow fields are derived from a publicly available dataset, encompassing diverse types of flows as described in (Cai et al., 2019). Then, our simulator disperses particles within a given flow field, generating a high-frame-rate particle flow video (Raffel et al., 2018). The event data can be extracted from the video, while simultaneously, images at fixed time intervals are selected for PIV analysis. The primary contributions are as follows:

- A particle frame/event generator. We provide an integrated tool that synthesizes particle image sequences and event stream data based on a specified velocity field. The generator is highly customizable, allowing users to adjust key parameters such as particle density and event triggering thresholds to meet diverse data generation requirements.
- A dual-modal dataset. The dataset—integrating particle images, events, and ground truth flow fields—is released. The dataset includes nine distinct flow field types and has a total size of 350GB, making it one dual-modal dataset available for advanced particle-based velocimetry.

2 Methods for Dataset Generation

2.1 Overview of Our Dataset

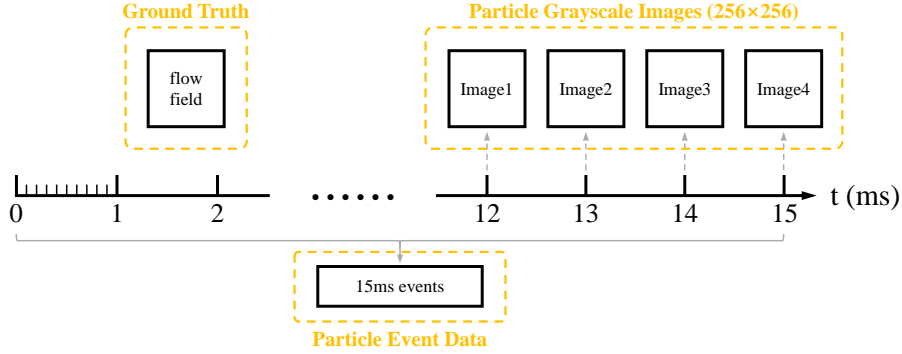


Figure 1: Timing diagram for FED-PV.

This section details the structure of the released dataset and the computational methods used for data generation, with particular emphasis on the technical implementation. Our dataset is based on the widely used dataset in the field of Particle Image Velocimetry (PIV) (Cai et al., 2019), which includes nine distinct flow field types with diverse dynamics. Building upon the work of Cai et al., we redefined the particle velocity units to meet the requirements for event data recording. For each flow field, event data was recorded over a duration of 15 ms, with the final 4 grayscale images preserved at 1 ms intervals (each image represents a snapshot of the corresponding moment). The timeline in Figure 1 provides a detailed explanation of the temporal sequence of particle image generation and event data acquisition.

2.2 The Image Generation Method

We utilized the CFD flow motion patterns from a publicly available dataset (Cai et al., 2019) as the ground truth benchmark. The static characteristics of particles are modeled using a two-dimensional(2D) Gaussian function, where the intensity distribution of each particle is represented as:

$$I(x, y) = I_0 \exp \left[\frac{-(x - x_0)^2 - (y - y_0)^2}{(1/8) d_p^2} \right] \quad (1)$$

where (x_0, y_0) represents the center position of particle, I_0 denotes the peak intensity at the Gaussian center, and d_p is the diameter of particle. The parameters are randomly sampled from predefined normal distributions during initialization, with a particle spatial density set at 0.06 particles per pixel (ppp).

To enhance image quality over long time spans, particularly at the domain boundaries, the computational domain is expanded from the original 256×256 flow field to a 288×288 spatial region using the smoothing algorithm (Lee et al., 2017a; Garcia, 2010).

The generation of particle grayscale images follows the Particle Image Generator (PIG) standard (Raffel et al., 2018), producing image sequences at fixed 1ms intervals using an iterative process. The final dataset retains the last four frames of the PIV image sequence. Within the iterative process, computations are performed using a minimal time step of $0.02ms$, during which particle motion is approximated as uniform linear movement. The velocity of each particle is equal to the local flow velocity at its position, which is obtained via bilinear interpolation.

To maintain the continuity of particle distribution within the camera window over extended time spans, a dynamic management mechanism for edge sub-regions is introduced at the computational domain boundaries. Figure 2 provides an overview of the computational domain. When the average brightness of an edge sub-region falls below a predefined threshold, new particles are introduced to simulate a continuous influx at a constant density. Meanwhile, to optimize computational efficiency, particles that exceed the computational domain are automatically removed.

2.3 The Event Generation Method

Event data is one of the core components of the entire dataset. We extract the brightness information of each pixel from a high-frame-rate image stream to simulate the operation of an event camera (Muegler et al., 2017; Rebecq et al., 2018). The event generation process is illustrated in the figure (Fig. 3).

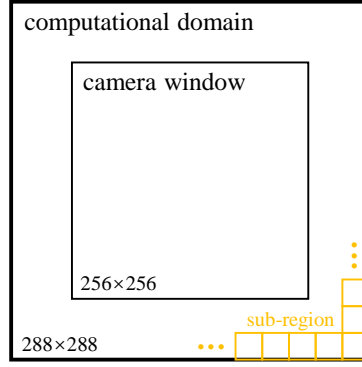


Figure 2: Definition of the computational domain of the flow field.

The x -axis represents the reading time of each frame of the image, while the y -axis indicates the brightness change of a specific pixel. The blue dashed line represents the actual brightness variation, and the yellow solid line shows the piecewise linear fit of the brightness for each frame of the image. C is the threshold, and an event is generated when the brightness change satisfies the following condition:

$$|\log(x, y, t_1) - \log(x, y, t_2)| \geq C \quad (2)$$

where x, y represents the pixel position, t represents time, and C is the threshold. A positive event is generated when the brightness change exceeds the threshold, while a negative event is generated when the brightness change is below the threshold.

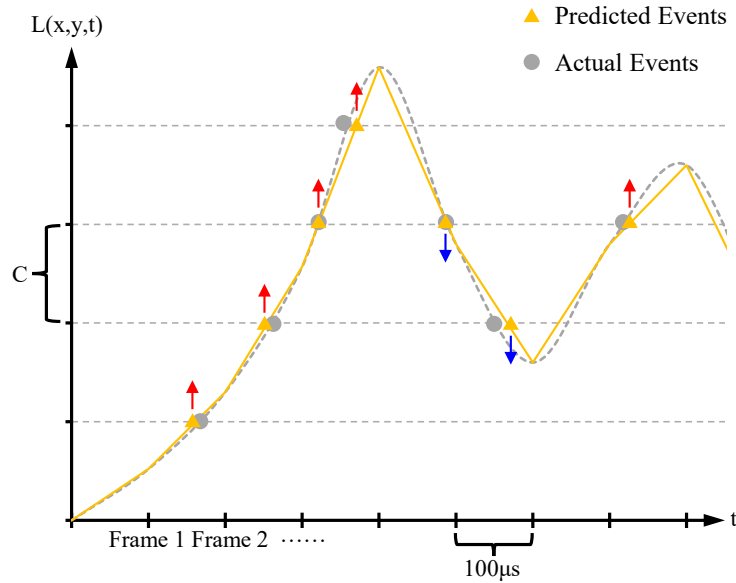


Figure 3: The Principle of Event Data Generation for the Dataset

Typically, the threshold C for event cameras is set within the range of 10% to 50% of the brightness change. A lower threshold results in a high density of events, but this also increases noise interference. On the other hand, a higher threshold effectively suppresses noise, but it also leads to a decrease in event count, which may hinder the detection of subtle changes. Since our dataset does not include noise, we have empirically selected a balanced threshold of 25%, where events are triggered when the brightness change exceeds this value. For those interested in exploring the optimal threshold selection, readers can test it themselves using our open-source code.

To ensure that high-frame-rate image data can accurately capture the motion trajectory of each particle, our dataset adopts an inter-frame interval of $100\mu s$. Given that particle velocities in the dataset typically range from 3 to 9 pixels/ms , the displacement between two consecutive frames does not exceed 1 pixel . This enables precise recording of the brightness variations across individual pixel locations traversed by the particles, significantly improving the accuracy of linear interpolation and thereby ensuring high precision in event data generation.

2.4 Details of a released Dataset

The dataset is categorized into 9 subsets based on the dynamic characteristics of flow fields, each corresponding to a distinct type of velocity field (the subset names are strictly aligned with the respective velocity field types). Within subsets, multiple scenarios are provided, each characterized by different flow field parameters and initial conditions. A scenario comprises four types of data: (1) Ground-truth velocity fields (stored in *.flo* format with units in pixel/s); (2) PIV images, comprising four sequential frames; (3) Event stream data (stored in *.h5* format). All images are single-channel grayscale images (*.png* format) with 256×256 pixel resolution. A comprehensive overview of the quantity and size of the dataset is presented in Table 1. Compared to the dataset by Cai et al., our dataset contains a greater number of particle grayscale images and includes a substantial amount of event-based data.

Table 1: Dataset scale information

Flow type	Quantity	Average velocity (<i>pixel/ms</i>)	Average number of events	Size
backstep	3600	1.8 – 4.4	6.13×10^6	94G
cylinder	2050	0.9 – 1.8	2.61×10^6	27G
DNS turbulence	2000	0.2 – 2.9	2.88×10^6	29G
JHTDB_channel	1900	0.8 – 6.7	8.92×10^6	81G
JHTDB_channel_hd	600	0.2 – 1.0	1.22×10^6	3.9G
JHTDB_isotropic1024_hd	2000	0.3 – 5.6	2.83×10^6	28G
JHTDB_mhd1024_hd	800	0.4 – 3.5	3.17×10^6	13G
SQG	1500	1.3 – 1.8	3.46×10^6	26G
uniform	1000	0.1 – 8.3	1.00×10^7	48G

3 Benchmarking of the Dataset

In this section, we evaluate the reliability and usability of our dataset using three mainstream PIV algorithms and three event-based algorithms. Based on these methods, we establish a benchmark on our dataset to provide a reference for future research and facilitate its application by other users.

3.1 PIV Application

To evaluate the quality of the image data generated in our dataset, we conducted tests using three representative methods: UnLiteFlowNet-PIV (Zhang and Piggott, 2020), Cross-correlation-PIV (Liberzon et al., 2016), and RAFT-PIV (Teed and Deng, 2020). The images used in all tests were Image1 and Image2 for each flow field (corresponding to the flow fields at 12ms and 13ms, respectively), with an image resolution of 256×256 .

Figure 5 presents the testing results of the six flow fields using the three aforementioned methods. Overall, all three methods are capable of reasonably reconstructing the underlying flow structures. Specifically, the UnLiteFlowNet-PIV method exhibits noticeable discontinuities in the estimated flow, such as abrupt changes in the bottom-right corner of JHTDB_channel_hd_00285. The Cross-correlation-PIV method, while limited in resolution due to its inherent computational constraints, still captures the general flow patterns present in the dataset. RAFT-PIV, as a well-established baseline, produces consistently high-quality results with superior accuracy. These observations align well with existing knowledge in the PIV research community and further demonstrate the reliability of our dataset for PIV-based flow analysis.

In addition, we adopt three commonly used evaluation metrics in the PIV domain—RMSE, AEE, and AAE—to establish a benchmark for our dataset. Table 2 presents the statistical characteristics of these metrics across nine types of flow fields in our dataset, evaluated using UnLiteFlowNet-PIV, Cross-correlation-PIV, and RAFT-PIV. For most flow fields, the RMSE values of the three methods fall within the range of 0.1 to 0.3. However, in more complex flow scenarios, Cross-correlation-PIV tends to exhibit larger errors. We hope these results can serve as a useful reference for future algorithm development based on our dataset. Meanwhile, the notable room for improvement observed across multiple flow fields indicates that there remains significant potential for advancing high-performance PIV algorithms.

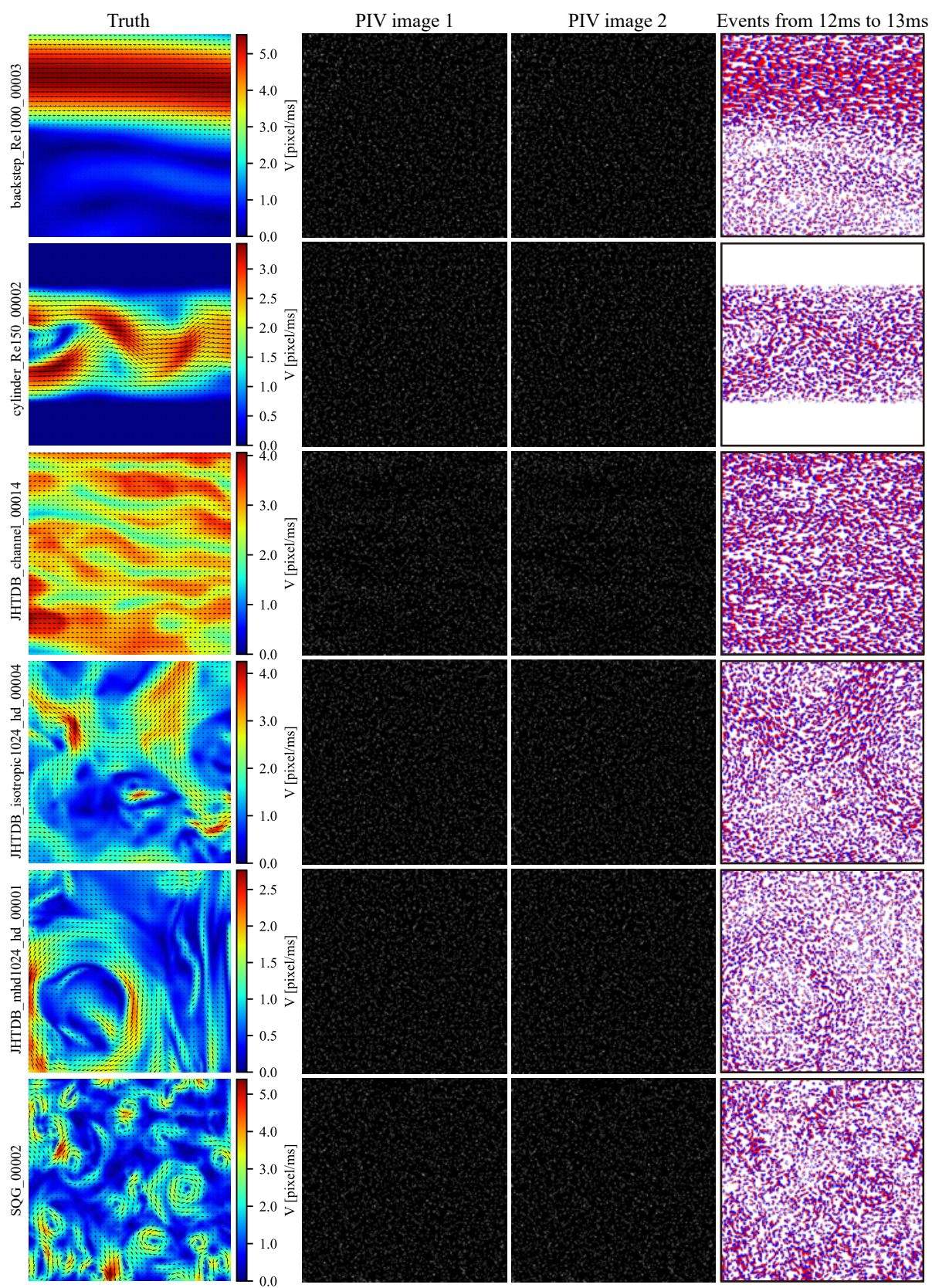


Figure 4: The visualization of our dataset.

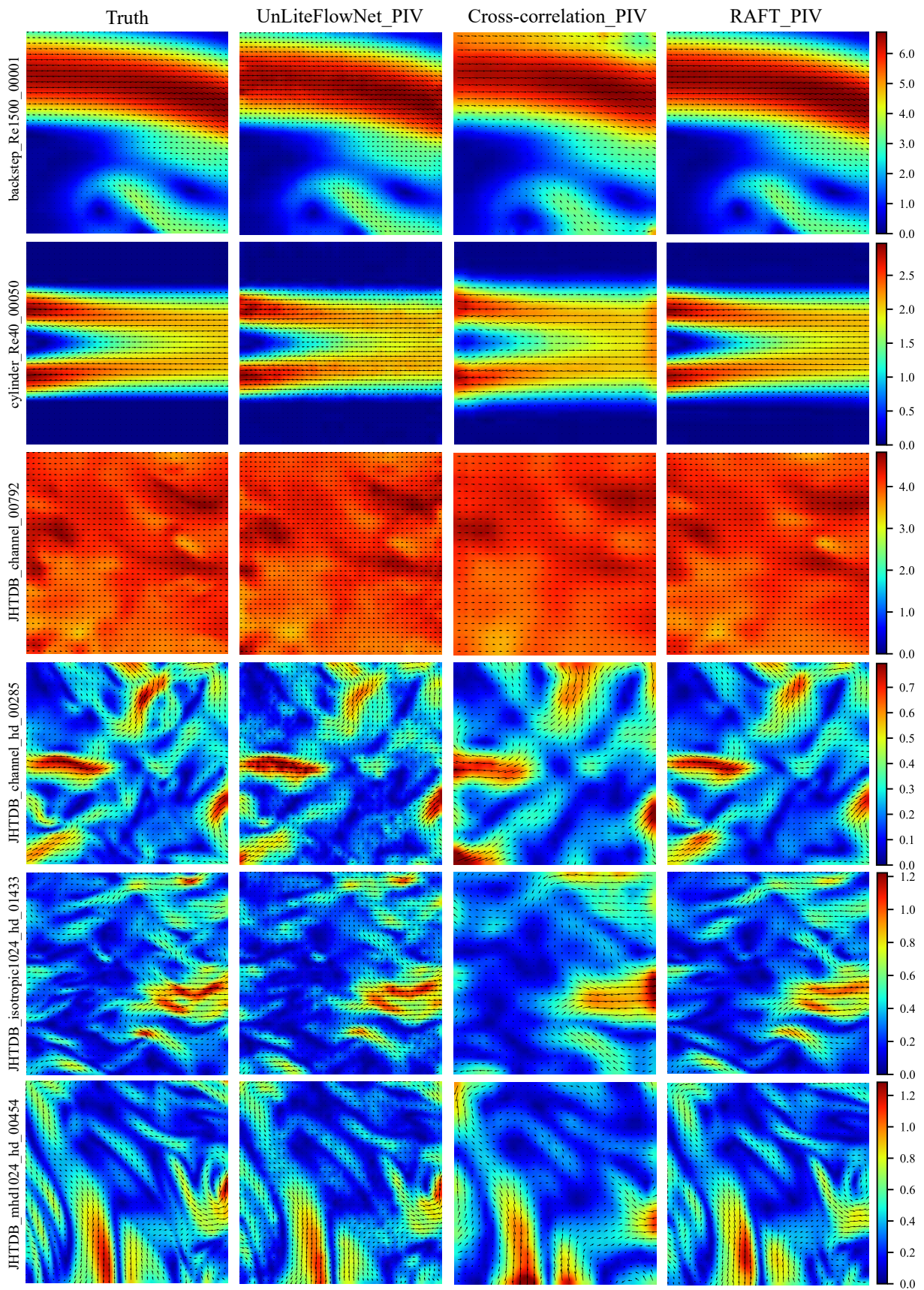


Figure 5: The visualization of PIV Application.

Table 2: Quantitative comparison of different PIV methods evaluated on our proposed dataset.

Flow type	Method	RMSE	AEE	AAE
backstep	UnLiteFlowNet_PIV	0.134	0.058	0.056
	Cross-correlation_PIV	0.201	0.101	0.033
	RAFT_PIV	0.167	0.107	0.030
cylinder	UnLiteFlowNet_PIV	0.075	0.058	0.683
	Cross-correlation_PIV	0.219	0.143	0.593
	RAFT_PIV	0.089	0.065	0.684
DNS_turbulence	UnLiteFlowNet_PIV	0.206	0.165	0.137
	Cross-correlation_PIV	1.037	0.807	0.577
	RAFT_PIV	0.218	0.163	0.111
JHTDB_channel	UnLiteFlowNet_PIV	0.147	0.095	0.018
	Cross-correlation_PIV	0.305	0.221	0.028
	RAFT_PIV	0.268	0.214	0.041
JHTDB_channel_hd	UnLiteFlowNet_PIV	0.089	0.073	0.129
	Cross-correlation_PIV	0.240	0.189	0.304
	RAFT_PIV	0.122	0.100	0.186
JHTDB_isotropic1024_hd	UnLiteFlowNet_PIV	0.157	0.119	0.097
	Cross-correlation_PIV	0.441	0.331	0.249
	RAFT_PIV	0.336	0.252	0.176
JHTDB_mhd1024_hd	UnLiteFlowNet_PIV	0.154	0.118	0.083
	Cross-correlation_PIV	0.479	0.341	0.214
	RAFT_PIV	0.339	0.242	0.152
SQG	UnLiteFlowNet_PIV	0.231	0.184	0.111
	Cross-correlation_PIV	1.059	0.735	0.388
	RAFT_PIV	0.197	0.145	0.068
uniform	UnLiteFlowNet_PIV	1.183	0.677	0.134
	Cross-correlation_PIV	0.179	0.089	0.010
	RAFT_PIV	1.828	1.749	0.362

3.2 Event-based Imaging Velocimetry Application

To evaluate the quality of the generated event data, we employed three representative methods: EBIV (Willert and Klinner, 2022), E-RAFT (Gehrig et al., 2021b), and Contrast-Maximization (Gallego et al., 2018). For all three methods, we utilized the complete set of event data collected within a 15ms time window.

Figure 6 shows the evaluation results of six different flow field datasets. Overall, the tested methods are able to reconstruct the basic characteristics of the flow fields. Among them, the EBIV method performs relatively well, but still exhibits distortions in event-sparse regions—for instance, outliers appear in the upper region of cylinder_Re300_00351. As for E-RAFT, due to the lack of algorithmic tuning in our experiments, its performance is suboptimal. Nevertheless, the results highlight the great potential of deep learning networks in processing event-based information. In contrast, the Contrast-Maximization method suffers from long computation times and limited accuracy. As shown in the figure, when the computational grid is coarse, it can only roughly capture the overall flow pattern and fails to estimate high-speed motion accurately, such as in backstep_Re1000_00035. Overall, We hope this dataset can serve as a strong foundation for developing faster and more accurate algorithms, particularly for event-driven deep learning approaches.

Similarly, the Table 3 summarizes the detailed statistical evaluation metrics of the three aforementioned methods. Overall, EBIV demonstrates higher computational accuracy than E-RAFT, and in some cases, its performance approaches that of PIV-based methods. Contrast-Maximization still has significant room for improvement: while its performance is relatively close to the other two methods in low-velocity flow fields, it falls short in high-speed scenarios. These evaluation metrics provide valuable benchmarks for developing event-based velocity estimation algorithms using our dataset. Furthermore, they point to a promising research direction—fusing image and event-based data to enhance computational accuracy through multimodal information integration.

4 Conclusion

In this paper, we propose FED-PV, a bimodal data generation framework. By incorporating an extended computational domain and minimal iterative step design, FED-PV achieves high-fidelity modeling of particle motion under a steady flow field. Based on this framework, we construct an open-source dataset comprising 9 typical flow field categories with a total size of 350GB. Through systematic evaluations using multiple PIV and PEV algorithms, we provide key performance metrics of the dataset (RMSE, AEE and AAE) across a range of mainstream particle velocimetry methods. Given the current lack of research on multimodal particle velocimetry, the open-source framework and the accompanying dataset we provide (project repository: <https://github.com/DreamFuture6/FED-PV>) serve as a valuable resource to support future studies in high-performance multimodal particle velocimetry.

Acknowledgements

We would like to thank Jeremiah Hu and Wang Wei for providing support with the RAFT-PIV data used in this work. We would like to thank PhD candidate Jia Ai for the valuable discussions and helpful suggestions on the experimental design and methodology. We also express our gratitude to the ISPIV organizing committee. This work was supported by the Hubei Provincial Natural Science Foundation of China (Grant No. 2023AFB128).

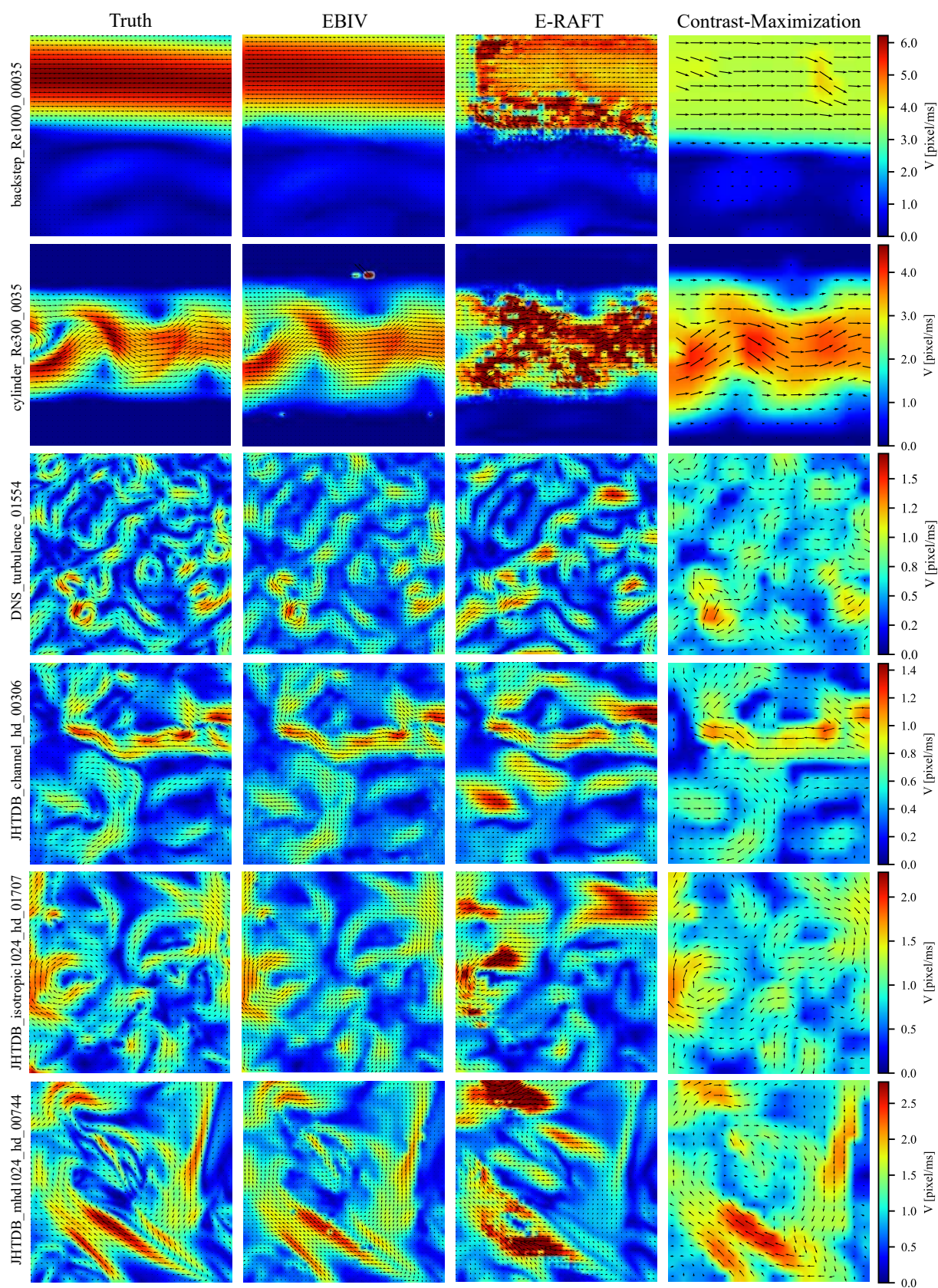


Figure 6: The visualization of Event Application.

Table 3: Quantitative comparison of different event methods evaluated on our proposed dataset.

Flow type	Method	RMSE	AEE	AAE
backstep	EBIV	0.249	0.194	0.114
	E-RAFT	0.851	0.747	0.266
	Contrast-Maximization	1.236	0.876	0.216
cylinder	EBIV	0.591	0.165	0.647
	E-RAFT	0.972	0.765	0.895
	Contrast-Maximization	0.484	0.318	0.699
DNS_turbulence	EBIV	0.632	0.486	0.301
	E-RAFT	0.297	0.249	0.405
	Contrast-Maximization	0.854	0.682	0.422
JHTDB_channel	EBIV	0.203	0.165	0.019
	E-RAFT	0.681	0.591	0.293
	Contrast-Maximization	0.758	0.671	0.067
JHTDB_channel_hd	EBIV	0.122	0.092	0.183
	E-RAFT	0.224	0.192	0.273
	Contrast-Maximization	0.303	0.234	0.365
JHTDB_isotropic1024_hd	EBIV	0.290	0.202	0.150
	E-RAFT	0.418	0.301	0.326
	Contrast-Maximization	0.513	0.406	0.307
JHTDB_mhd1024_hd	EBIV	0.310	0.199	0.128
	E-RAFT	0.507	0.392	0.373
	Contrast-Maximization	0.597	0.448	0.287
SQG	EBIV	0.795	0.561	0.307
	E-RAFT	1.112	0.997	0.874
	Contrast-Maximization	0.905	0.719	0.344
uniform	EBIV	0.061	0.060	0.005
	E-RAFT	0.048	0.041	0.003
	Contrast-Maximization	0.977	0.910	0.104

References

- Ai J, Chen Z, Li J, and Lee Y (2025a) Rethinking asymmetric image deformation with post-correction for particle image velocimetry. *Physics of Fluids* 37
- Ai J, Chen Z, Ning W, and Lee Y (2025b) A projection concentration maximization method for event-based imaging velocimetry. in *16th International Symposium on Particle Image Velocimetry (ISPIV 2025)*
- AlSattam O, Mongin M, Grose M, Gunasekaran S, and Hirakawa K (2024) Kf-pev: a causal kalman filter-based particle event velocimetry. *Experiments in Fluids* 65:141
- Cai S, Zhou S, Xu C, and Gao Q (2019) Dense motion estimation of particle images via a convolutional neural network. *Experiments in Fluids* 60:1–16
- Gallego G, Rebecq H, and Scaramuzza D (2018) A unifying contrast maximization framework for event cameras, with applications to motion, depth, and optical flow estimation. in *Proceedings of the IEEE Conference on Computer Vision and Pattern Recognition (CVPR)*
- Garcia D (2010) Robust smoothing of gridded data in one and higher dimensions with missing values. *Computational Statistics & Data Analysis* 54:1167–1178
- Gehrig M, Aarents W, Gehrig D, and Scaramuzza D (2021a) Dsec: A stereo event camera dataset for driving scenarios. *IEEE Robotics and Automation Letters* 6:4947–4954
- Gehrig M, Millhäusler M, Gehrig D, and Scaramuzza D (2021b) E-raft: Dense optical flow from event cameras. in *2021 International Conference on 3D Vision (3DV)*. pages 197–206
- Kähler CJ, Scharnowski S, and Cierpka C (2012) On the resolution limit of digital particle image velocimetry. *Experiments in fluids* 52:1629–1639
- Lee Y, Gu F, Gong Z, Pan D, and Zeng W (2024) Surrogate-based cross-correlation for particle image velocimetry. *Physics of Fluids* 36
- Lee Y and Mei S (2021) Diffeomorphic particle image velocimetry. *IEEE Transactions on Instrumentation and Measurement* 71:1–10
- Lee Y, Yang H, and Yin Z (2017a) Outlier detection for particle image velocimetry data using a locally estimated noise variance. *Measurement Science and Technology* 28:035301
- Lee Y, Yang H, and Yin Z (2017b) Piv-dcnn: cascaded deep convolutional neural networks for particle image velocimetry. *Experiments in Fluids* 58:171
- Liberzon A, Lasagna D, Aubert M, Bachant P, jakirkham, ranleu, and Borg J (2016) Openpiv/openpiv-python: Updated pyprocess with extended area search method
- Mueggler E, Rebecq H, Gallego G, Delbruck T, and Scaramuzza D (2017) The event-camera dataset and simulator: Event-based data for pose estimation, visual odometry, and slam. *The International Journal of Robotics Research* 36:142–149
- Ohmi K and Li HY (2000) Particle-tracking velocimetry with new algorithms. *Measurement Science and Technology* 11:603
- Raffel M, Willert CE, Scarano F, Kähler CJ, Wereley ST, and Kompenhans J (2018) *Particle image velocimetry: a practical guide*. springer
- Rebecq H, Gehrig D, and Scaramuzza D (2018) Esim: an open event camera simulator. in *Conference on robot learning*. pages 969–982. PMLR
- Teed Z and Deng J (2020) Raft: Recurrent all-pairs field transforms for optical flow. in *Computer Vision—ECCV 2020: 16th European Conference, Glasgow, UK, August 23–28, 2020, Proceedings, Part II* 16. pages 402–419. Springer
- Wan Z, Mao Y, Zhang J, and Dai Y (2023) Rpeflow: Multimodal fusion of rgb-pointcloud-event for joint optical flow and scene flow estimation. in *Proceedings of the IEEE/CVF International Conference on Computer Vision*. pages 10030–10040

- Willert CE and Klinner J (2022) Event-based imaging velocimetry: an assessment of event-based cameras for the measurement of fluid flows. *Experiments in Fluids* 63:101
- Zhang M and Piggott MD (2020) Unsupervised learning of particle image velocimetry. in *High Performance Computing: ISC High Performance 2020 International Workshops, Frankfurt, Germany, June 21–25, 2020, Revised Selected Papers* 35. pages 102–115. Springer
- Zhu AZ, Thakur D, Özaslan T, Pfrommer B, Kumar V, and Daniilidis K (2018) The multivehicle stereo event camera dataset: An event camera dataset for 3d perception. *IEEE Robotics and Automation Letters* 3:2032–2039